Chemical Interactions Between Ship-Originated Air Pollutants and Ocean-Emitted Halogens

Qinyi Li[1] , Alba Badia[2] , Rafael P. Fernandez[1,3] , Anoop S. Mahajan[4] , Ana Isabel López-Noreña[5] , Yan Zhang[6] , Shanshan Wang[6], Enrique Puliafito[5] , Carlos A. Cuevas[1] , and Alfonso Saiz-Lopez[1]

[1]Department of Atmospheric Chemistry and Climate, Institute of Physical Chemistry Rocasolano, CSIC, Madrid, Spain, [2]Institute of Environmental Science and Technology (ICTA), Universitat Autònoma de Barcelona (UAB), Barcelona, Spain, [3]Institute for Interdisciplinary Science (ICB), National Research Council (CONICET), FCEN-UNCuyo, Mendoza, Argentina, [4]Centre for Climate Change Research, Indian Institute of Tropical Meteorology, Pune, India, [5]Atmospheric and Environmental Studies Group (GEAA), National Technological University (UTN-FRM), CONICET, Mendoza, Argentina, [6]Department of Environmental Science and Engineering, Shanghai Key Laboratory of Atmospheric Particle Pollution and Prevention, Fudan University, Shanghai, China

Abstract Ocean-going ships supply products from one region to another and contribute to the world's economy. Ship exhaust contains many air pollutants and results in significant changes in marine atmospheric composition. The role of reactive halogen species (RHS) in the troposphere has received increasing recognition and oceans are the largest contributors to their atmospheric burden. However, the impact of shipping emissions on RHS and that of RHS on ship-originated air pollutants have not been studied in detail. Here, an updated Weather Research Forecasting coupled with Chemistry model is utilized to explore the chemical interactions between ship emissions and oceanic RHS over the East Asia seas in summer. The emissions and resulting chemical transformations from shipping activities increase the level of NO and NO_2 at the surface, increase O_3 in the South China Sea, but decrease O_3 in the East China Sea. Such changes in pollutants result in remarkable changes in the levels of RHS (>200% increase of chlorine; ~30% and ~5% decrease of bromine and iodine, respectively) as well as in their partitioning. The abundant RHS, in turn, reshape the loadings of air pollutants (~20% decrease of NO and NO_2; ~15% decrease of O_3) and those of the oxidants (>10% reduction of OH and HO_2; ~40% decrease of NO_3) with marked patterns along the ship tracks. We, therefore, suggest that these important chemical interactions of ship-originated emissions with RHS should be considered in the environmental policy assessments of the role of shipping emissions in air quality and climate.

1. Introduction

Shipment is the dominant method for redistributing products from one continent to another and is critical in sustaining the world's economy. Shipping activities result in emissions of air pollutants over natural waters and contribute approximately 15% of the NO_x emissions and 13% of the SO_x emissions on a global scale (IMO, 2014; Kontovas, 2020).

Ship-originated air pollutants (primary emissions and their secondary products) have been reported to affect the atmospheric composition, air quality, and human health. A pioneering study by Lawrence and Crutzen (1999) revealed that ship emissions reshape atmospheric chemistry in the marine boundary layer (MBL). Eyring et al. (2010) reported that ship emissions of air pollutants caused air quality problems with elevated nitrogen oxides, sulfur, particulate matter, and ground-level ozone (O_3) in coastal areas and harbors. Fan et al. (2016) and Lv et al. (2018) also suggested that ship emissions have a noticeable influence on air quality in East China and East Asia, respectively. The reduced air quality due to ship emissions can lead to adverse health impacts with 14,500–37,500 worldwide premature deaths per year (H. Liu et al., 2016). Ship emissions affect climate via their effects on greenhouse gases (CO_2, CH_4, and O_3) and cloud condensation nuclei (Von Schneidemesser et al., 2015). Ship emissions also change marine stratocumulus regime of open cells into closed cells inducing negative radiative forcing (Y.-C. Chen et al., 2012; Goren & Rosenfeld, 2012).

The budget of reactive halogen species (RHS) can also be influenced by shipping emissions. Osthoff et al. (2008) reported the first ambient measurement of $ClNO_2$, an important reservoir of reactive chlorine,

and linked its production with ship plumes and coastal pollution. Ship-emitted NO_x (=NO + NO_2) and SO_2 increase the deposition of acids (HNO_3, H_2SO_4) to the sea surface and aerosols, decreasing their pH, which can potentially affect the debromination process of sea-salt aerosols (Badia et al., 2019; Yang et al., 2005). This emitted NO_x also affects the formation of O_3 and hence the subsequent emission of iodine species (I_2 and HOI) from the oxidation of iodide in seawater (Carpenter et al., 2013; Macdonald et al., 2014), transforms reactive halogen oxides into halogen nitrates which ultimately deposit onto the sea surface (Simpson et al., 2015), and is associated with nighttime iodine chemistry (Saiz-Lopez et al., 2016), for example, via the reaction of NO_3 with both I_2 and HOI.
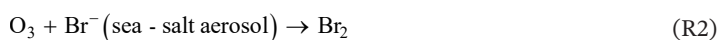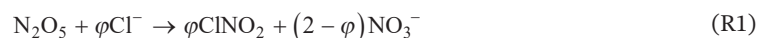
Oceans are the largest source of reactive halogen (Cl, Br, and I) species and most of the impact of oceanic halogens inherently occurs in the marine atmosphere (Simpson et al., 2015). Reactive halogens change the partitioning of HO_2 and OH which affects the oxidation capacity of the atmosphere (Li, Badia, Wang, et al., 2020), as well as the partitioning of NO and NO_2 and hence affects the air quality (Li et al., 2019; Sherwen et al., 2017). Reactive halogens increase the loss of O_3 (via reactions of halogen atoms with O_3) and reduce the production of O_3 (via the reactions of halogen oxides with NO_2), which affects air quality and radiative forcing (Hossaini et al., 2015; Saiz-Lopez et al., 2012, 2014; Sherwen, et al., 2016; Sherwen, Schmidt, et al., 2016). Halogen-mediated tropospheric ozone loss is also linked to climate and is projected to be a key component of the ozone budget throughout the 21st century (Iglesias-Suarez et al., 2020). Halogen atoms (mostly chlorine but also bromine atoms) also react with volatile organic compounds (VOCs) and initiate photochemical production of O_3 in polluted areas (Li et al., 2016; Sarwar et al., 2012).

This work focuses on evaluating the interaction of ship-originated air pollutants and atmospheric halogens emitted from the ocean. We adopt a revised regional chemical transport model, Weather Research Forecasting coupled with Chemistry (WRF-Chem), updated with comprehensive implementation of halogen sources and chemistry (Badia et al., 2019) and the EDGAR emission inventory for air pollutants from ship-ment activities (Crippa et al., 2018), to look into the interaction between ship-originated air pollutants and oceanic halogen emissions within the lower troposphere over the open ocean. We choose East Asia as the region of interest because (1) very few studies on reactive halogens have been conducted in this area; (2) this region contributes nearly 40% of the seaborne trade around the world (H. Liu et al., 2016); and (3) this region is one of the world's busiest ship tracks (Crippa et al., 2018).

2. Method and Materials

2.1. WRF-Chem Model

The halogen sources and chemistry incorporated in the WRF-Chem model have been documented in detail in Badia et al. (2019). Here, we briefly describe the main processes. A few heterogeneous reactions activate (relatively) inert halogen species (chloride, HCl, bromide in sea-salt aerosol, iodide in seawater, etc.) to reactive gaseous species (e.g., R1–R3). In R1, φ represents the $ClNO_2$ production branching ratio (yield).

$$N_2O_5 + \varphi Cl^- \rightarrow \varphi ClNO_2 + (2 - \varphi)NO_3^- \tag{R1}$$

$$O_3 + Br^- (\text{sea - salt aerosol}) \rightarrow Br_2 \tag{R2}$$

$$O_3 + I^- (\text{sea - water}) \rightarrow I_2 + HOI \tag{R3}$$

These halogens actively participate in atmospheric chemistry via (1) directly destroying O_3 molecule (R4); (2) oxidizing VOCs which contributes to the generation of more oxidants including RO_2, HO_2, OH, and O_3 (R5–R9); (3) perturbing the partitioning of HO_x (R10 and R11) and NO_x (R12); and (4) providing a sink for NO_x (R13) (Saiz-Lopez & von Glasow, 2012; Simpson et al., 2015). The loss of halogen species is primarily through deposition on aerosol and ground surface with halogen nitrates ($ClNO_3$, $BrNO_3$, and INO_3) having the highest Henry's law constants (Badia et al., 2019).

$$X + O_3 \rightarrow XO(X = Cl; Br; \text{and } I) \tag{R4}$$
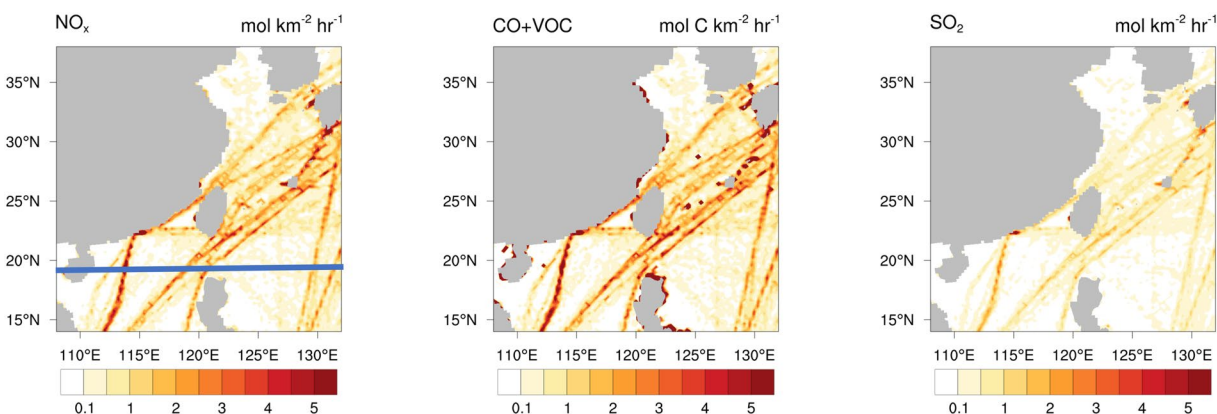
Figure 1. Emissions of NO_x, CO and VOC, and SO_2 (mol km^{-2} h^{-1}) over the ocean within the study domain. The blue line is used for further cross-section analysis.

$$Cl(Br) + VOC \rightarrow RO_2 + HCl(HBr) \tag{R5}$$

$$RO_2 + NO \rightarrow NO_2 + RO \tag{R6}$$

$$HO_2 + NO \rightarrow NO_2 + OH \tag{R7}$$

$$NO_2 + h\nu \rightarrow NO + O(^3P) \tag{R8}$$

$$O(^3P) + O_2 \rightarrow O_3 \tag{R9}$$

$$XO + HO_2 \rightarrow HOX \tag{R10}$$

$$HOX + h\nu \rightarrow X + OH \tag{R11}$$

$$XO + NO \rightarrow X + NO_2 \tag{R12}$$

$$XO + NO_2 \rightarrow XNO_3 \tag{R13}$$
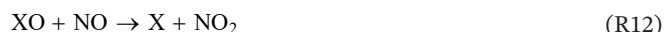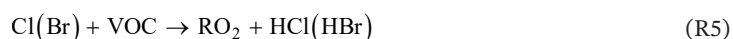
2.2. Emission Data

We follow Li, Badia, Wang, et al. (2020) to set up the reactive halogen scheme in order to calculate the reactive halogen emissions online. Although in the present study, we do not include the anthropogenic chlorine emission inventory over mainland China because the focus here is over the oceanic area.

We use the MEIC emission inventory (www.meicmodel.org) for routine air pollutants (NO_x, SO_2, CO, VOC, NH_3, $PM_{2.5}$, and PM_{10}) in mainland China and EDGARv4.3.2 emission inventory (Crippa et al., 2018) for air pollutants in other East Asian regions. For the ship emissions, the EDGARv4.3.2 inventory is adopted. Note that there are no halogen emissions in the EDGAR and MEIC emission inventories. The geographical distribution for ship emissions of NO_x, CO and VOCs, and SO_2 over the ocean is shown in Figure 1. We acknowledge that there have been a few emission inventories developed for East Asia with various spatial and temporal coverage, for example, Fan et al. (2016) for the year 2010, H. Liu et al. (2016) and Lv et al. (2018) for the year 2013, and D. Chen et al. (2017) for the year 2014. Please note that in the present conceptual

Table 1
Simulation Scenarios

Cases	Ship emission	Oceanic halogen emission	Halogen chemistry
NO-SHIP	No	Yes	Yes
NO-HAL	Yes	No	No
FULL	Yes	Yes	Yes

work, we investigate the coupled chemistry of ship emissions and oceanic halogens and we do not intend to characterize shipping emission inventories in East Asia.

2.3. Simulation Setup

The domain of interest (14°N–38°N, 108°E–132°E) is shown in Figure 1 and covers the coastlines of most East Asian regions. The simulation period is July 20, 2018 to August 31, 2018 considering the initial 11 days in July as model spin-up. Three simulation scenarios, as shown in Table 1, were conducted to identify the effects of the ship emissions on air pollutants and halogens (i.e., the changes between NO-SHIP and FULL cases) and those of halogens on ship-originated air pollutants (i.e., the difference of atmospheric composition between NO-HAL and FULL cases). Here, we note that we design our model simulations to quantify the sources (ship or oceanic halogen) and the corresponding subsequent chemical transformations on the atmospheric chemistry.

2.4. Model Performance Evaluation

We evaluated the simulated air pollutants and halogen species from the three cases with previously reported observations within (or close to) the domain of interest (Table S1). The reported average NO_2 ranges from 30 to 5,300 pptv (Lan et al., 2015; Schreier et al., 2015). The three scenarios also simulate a large concentration range (from pptv to ppbv levels) of NO_2 (see Section 3 for details). WRF-Chem simulations cover the range of NO_2 reported by the previous studies in this area but overestimate NO_2 compared to some studies and underestimate compared to others (Table S1). The discrepancy between model and measurements could be due to (1) different period between model and field campaigns; (2) different spatial dimensions and range (a single point in ground campaigns and a 3D line for flight campaigns compared to a 27×27 km^2 grid box in the model); (3) uncertainty in the emission inventory from shipping and the islands within the domain; and (4) missing sources and/or chemical mechanism of NO_x leading to the typical underestimation of NO_x levels in remote MBL by chemical transport models (e.g., Travis et al., 2020). Similarly, the present work reproduces the O_3 level in the South China Sea and Taiwan strait compared to one observation study (in average 21 ppbv) (Lan et al., 2015) but underestimates O_3 compared to other previous measurements (~50 to ~85 ppbv; Carmichael et al., 2003; Hatakeyama et al., 2004; Jacob et al., 2003). This could be due to (1) uncertainty in the emission inventories; (2) uncertainty in the initial and boundary conditions; (3) grid size and different spatial range; and (4) a lack of VOC emissions from the ocean (e.g., S. Wang, Hornbrook, et al., 2019). WRF-Chem underestimated CO compared to the observations with a range from 145 to 286 ppbv for CO (Carmichael et al., 2003; Jacob et al., 2003; Lan et al., 2015) (Table S1).

As to the loading of RHS in the region, previous studies reported a range of the daytime average of BrO from 0.15 to 1.7 pptv (Koenig et al., 2017) and a daytime average of IO from 0.4 to 1.4 pptv in the West Pacific (Großmann et al., 2013; Prados-Roman et al., 2015). The NO-SHIP scenario overestimates the level of BrO (daytime average of 0.96 pptv and maximum of 7.0 pptv at the surface) and IO (daytime average of 0.76 pptv and maximum of 1.6 pptv within MBL and 1.4 pptv and 4.2 pptv at the surface). The FULL case estimates an amount closer to the observations for both halogen oxides (daytime average of 0.45 pptv and maximum of 1.4 pptv for BrO at the surface; the daytime average of 0.68 pptv and maximum of 1.3 pptv of IO in MBL; and an average of 1.2 pptv and maximum of 2.6 pptv of IO at the surface; Table S1). A recent study (S. Liu et al., 2020) reported a wide range of mixing ratios of organic bromine species ($CHBr_3$, CH_2Br_2, and $CHBr_2Cl$) in the East China Sea and West Pacific. The present study underestimates these organic bromine species but covers the lower end of the measurements (Table S1). Note that these bromine species have a lifetime of tens to more than a hundred days (Fernandez et al., 2014) and therefore have limited impact on the bromine loading at the surface and within the MBL. In general, WRF-Chem reasonably reproduces the limited observations available over the Western Pacific.

3. Results and Discussion

3.1. Impact of Ship Emissions on Air Pollutants

The simulated average distribution of air pollutants (NO, NO_2, and O_3) at the surface for the NO-SHIP and FULL cases and the relative changes from NO-SHIP to FULL (the impact of ship emissions) are presented in Figure 2. Note that in the current study, we focus on the interaction between ship-originated air pollutants and oceanic halogens therefore we only present the results over the marine area. The reader is referred to Li, Badia, Wang, et al. (2020) for the influence of halogens on oxidation and air pollutants over land in this region.

In the NO-SHIP scenario, there are no emissions of NO_x over the ocean and the levels of NO (in average 12.3 pptv) and NO_2 (127.0 pptv) are low in most of the marine atmosphere (Figure 2). O_3 has an average mixing ratio of 19.9 ppbv and ranges between 10.0 and 50.0 ppbv over the ocean and peaks in the northern part of the domain which is affected by the outflow from China, Korea, and Japan (Figure 2).

In the FULL scenario, shipping activities add substantial (compared to the natural state of marine atmosphere) emissions of NO_x on top of this otherwise clean environment, which result in higher levels of NO (in average 38.3 pptv or 210.0% higher) and NO_2 (289.8 pptv or 128.0% higher) compared to the NO-SHIP scenario. Note that in the marine areas away from the coast, the NO_x enhancement near the ship tracks is as large as a factor of 10 (less than 10.0 pptv in NO-SHIP case as compared over 100.0 pptv in FULL case). The enhancement of NO_x levels results in an opposite impact on background ozone levels depending on location: O_3 is reduced in the northern part of the domain (East China Sea) by as much as -15.8% and enhanced in the southern part (South China Sea) up to 22.8% compared to the NO-SHIP scenario. This is because as a secondary product of photochemistry, O_3 has a nonlinear relationship with its precursors, NO_x and CO + VOCs (Seinfeld & Pandis, 2006). Thus, an increase of NO_x leads to (1) an increase of O_3 if the levels of CO in the NO-SHIP scenario are sufficient (e.g., >70 ppbv in the South China Sea) or (2) a decrease in O_3 if the levels of CO are lower (e.g., <60 ppbv in the East China Sea, Figure S1).

Most of the previous studies on the role of shipping activities in East Asia have focused on their impact on air quality over land (e.g., H. Liu et al., 2016; Z. Liu et al., 2017; Lv et al., 2018; Zhang et al., 2017). A model study by R. Wang, Tie, et al. (2019) in the East China Sea reported a range of −5 to 30 μg m^{-3} (∼−2.5 to 15 ppbv) difference in O_3 over the ocean at a specific hour (14:00 on September 21, 2015) after the addition of ship emissions. Our simulations have a similar range of impacts (Figure 2) but a different spatial pattern, possibly due to the different simulation period, different emission inventory, and halogen chemistry used here but not in previous works (see Section 2 for Methods and Materials). Overall, it can be seen that the ship emissions substantially change the simulated level of air pollutants over the ocean.

### 3.2. Impact of Ship Emissions on the Loading of Halogens

The total inorganic chlorine (Cl_y), bromine (Br_y), and iodine (I_y) in the NO-SHIP and FULL cases and the relative changes due to ship emissions are presented in Figure 3. In the NO-SHIP case, the average levels of Cl_y (38.7 pptv), Br_y (2.8 pptv), and I_y (9.0 pptv) present a spatial distribution that generally correlates with the level of O_3, NO_x, and chloride (as an indication of sea-salt aerosol; Figure S2) because the activation of halogens from sea-salt aerosol and sea surface to the gaseous phase is strongly mediated by O_3, NO_x, and sea-salt aerosol (Saiz-Lopez & von Glasow, 2012; Simpson et al., 2015).

The large changes in air pollutants due to the addition of ship emissions induce a significant difference in the simulated levels of halogen species. The average Cl_y over the ocean within our domain increases to 139.3 pptv (or by 259.8%) in the FULL scenario. Note that shipping activities substantially increase the level of NO_x (Figure 2) and OH (Figure S3) which activates chlorine from (relatively) inert chloride in sea-salt aerosol to reactive chlorine gases, for example, $ClNO_2$, $ClNO_3$, HOCl, and Cl_2. For Br_y, the average is reduced to 1.9 pptv (or by 32.8%) in the FULL scenario. The large enhancement of NO_x transforms BrO into $BrNO_3$ which deposits onto the sea surface and hence reduces the total gaseous bromine. Regarding I_y, the mean level is decreased to 8.5 pptv (or by 6.1%) in the FULL case. The NO_x enhancement also contributes to changes in I_y by favoring the formation of INO_3, instead of HOI which dominates as iodine reservoir species
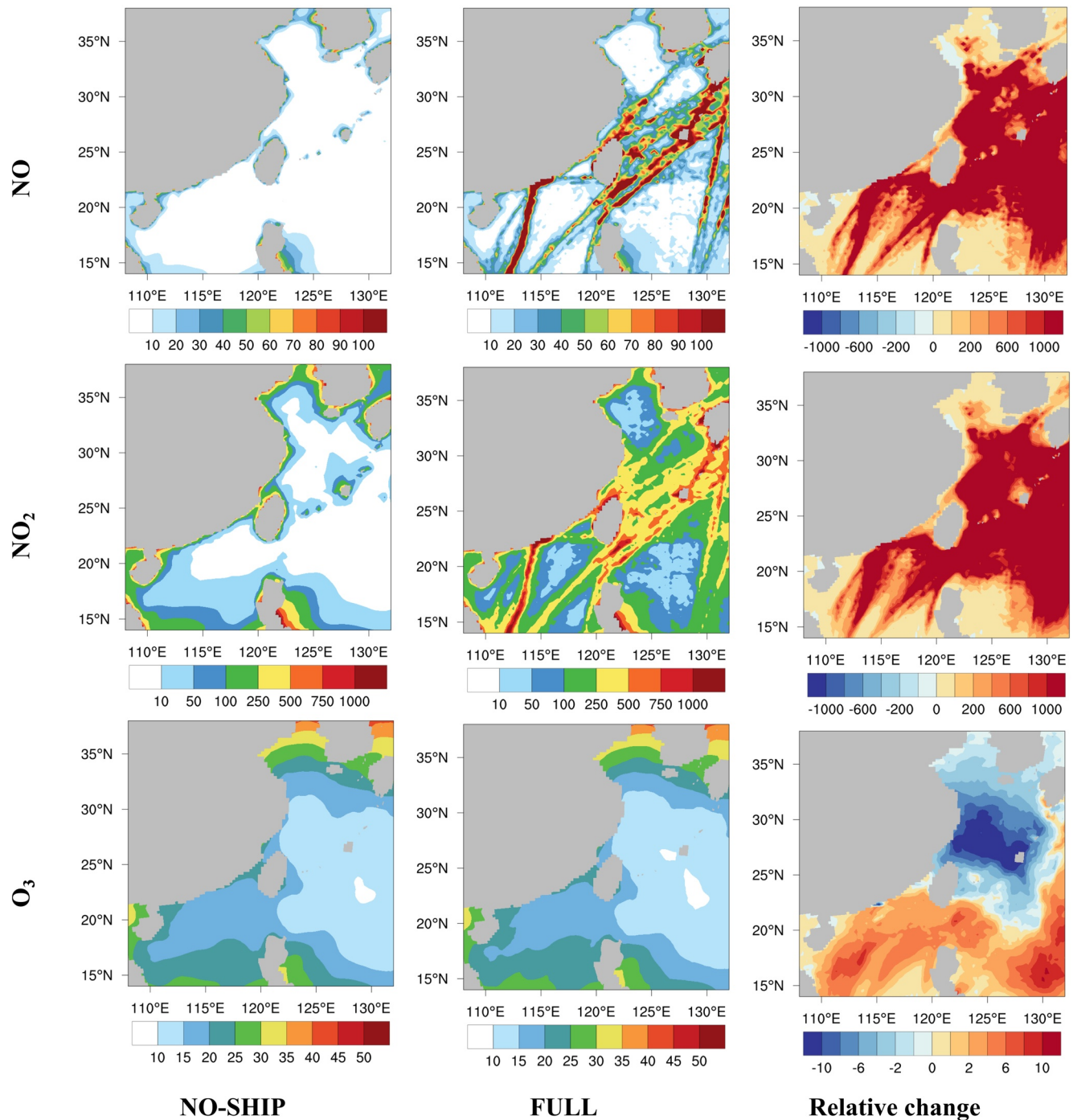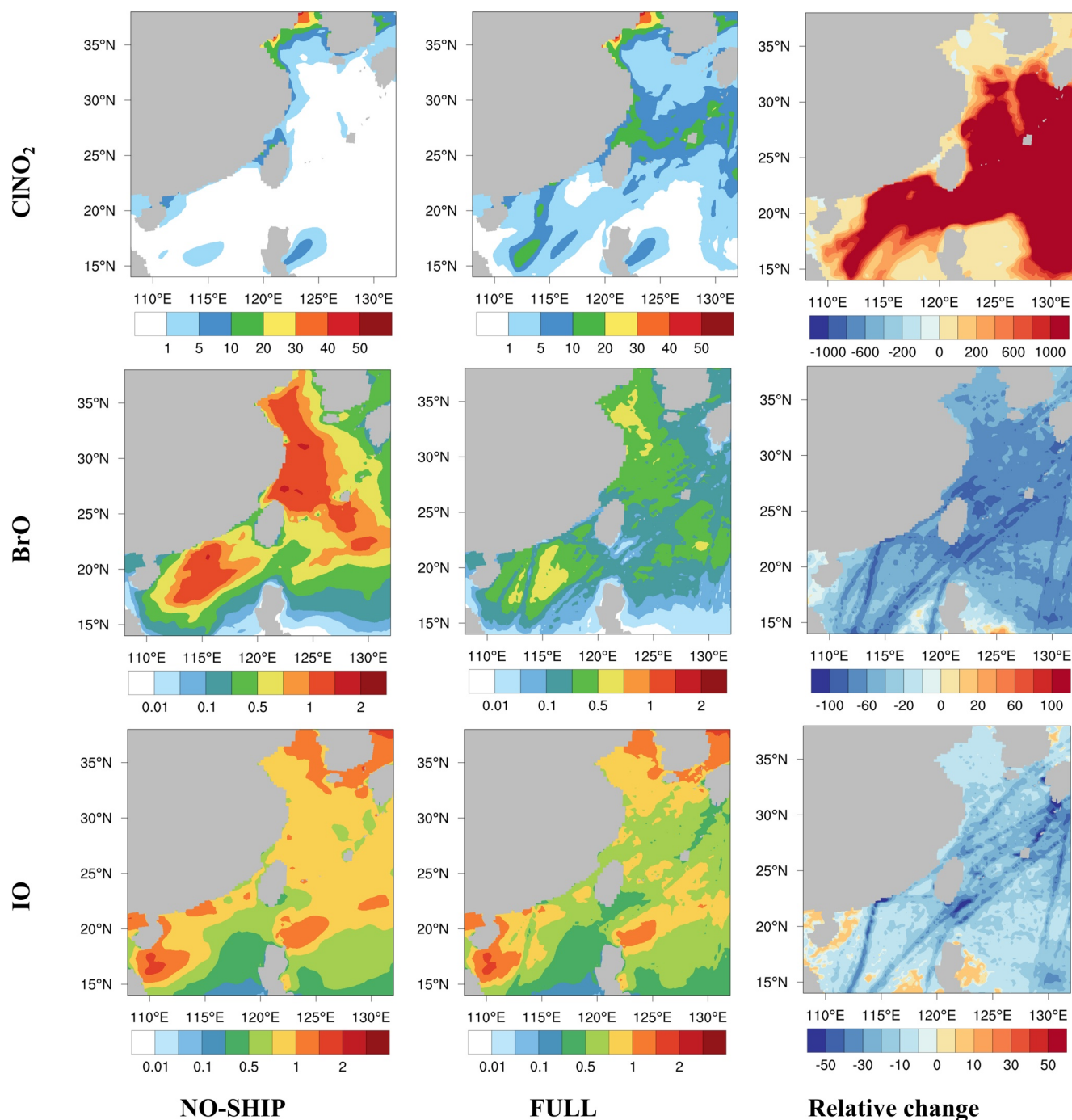
Figure 2. Simulated monthly average of NO (pptv, top), NO_2 (pptv, middle), and O_3 (ppbv, bottom) at the surface for the NO-SHIP (left) and FULL (center) scenarios. The relative change (in percentage) between scenarios is shown in the right column. The relative change of one species (here using NO as an example) between two cases in this paper is calculated as: $NO_{relativechange} = \left(NO_{FULL} - NO_{NO\text{-}SHIP} \right) / NO_{NO\text{-}SHIP} \times 100$.

in low NO_x environments. The reduction of O_3, in turn, decreases the emission of I_2 and HOI from the ocean (Carpenter et al., 2013; Macdonald et al., 2014). Simulated levels of halogens in the FULL scenario are in line with the results in Li, Badia, Wang, et al. (2020) except that the present study does not include anthropogenic chlorine emissions over the land and hence simulates lower levels of chlorine.
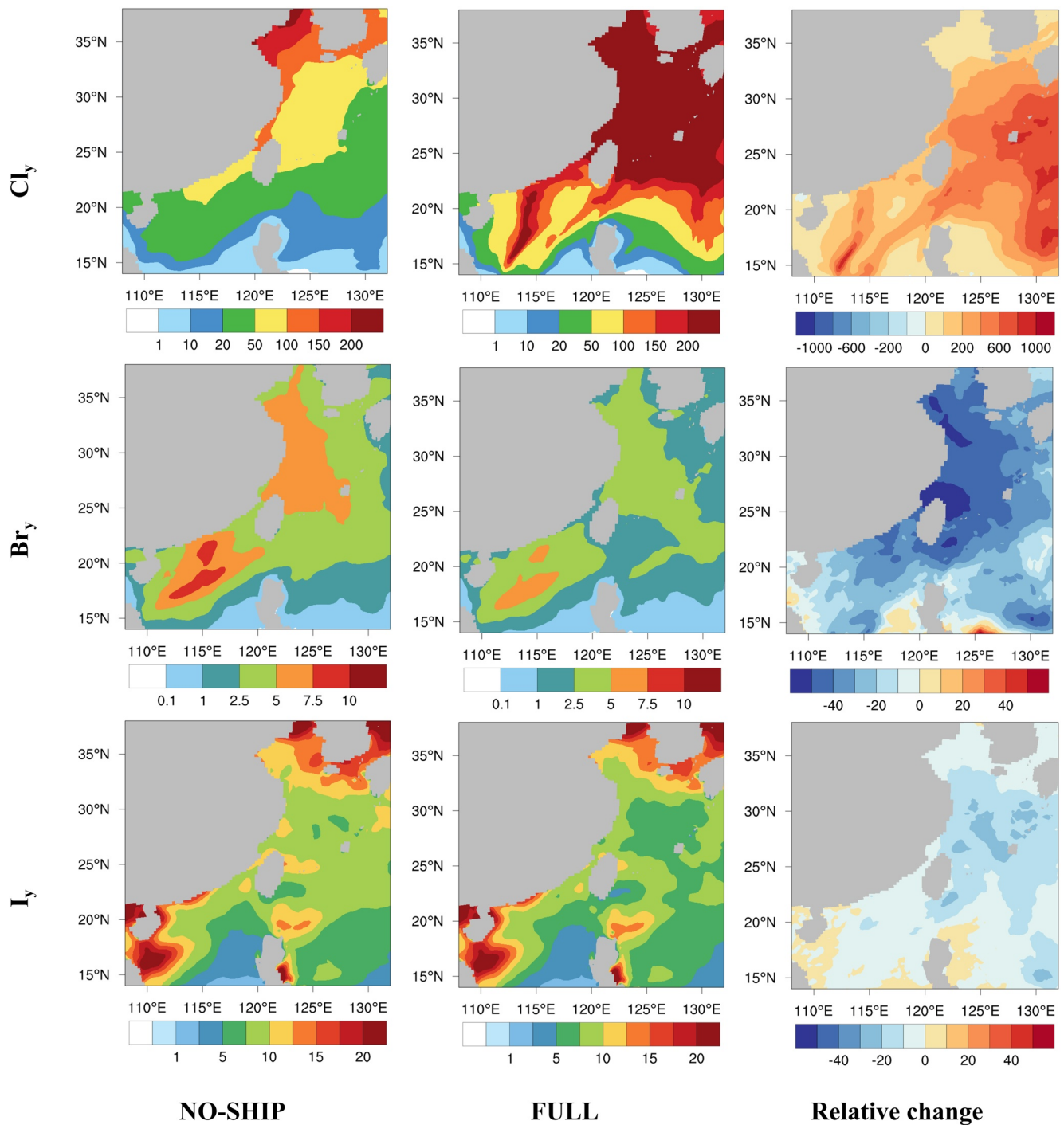
Figure 3. Simulated monthly average of Cl_y (pptv, top), Br_y (pptv, middle), and I_y (pptv, bottom) at the surface for the NO-SHIP (left) and FULL (center) scenarios. The relative change (in percentage) between scenarios is shown in the right column.

We now look at the effects of ship emissions on the featured species of reactive halogens, $ClNO_2$, BrO, and IO (Figure 4). Shipping activities increase the levels of NO_x and hence the production of $ClNO_2$. But for BrO, the large NO_x levels along the ship tracks rapidly transform BrO to $BrNO_3$, which is subsequently taken up on aerosols, therefore, decreasing the levels of BrO. As for IO, the ship-emitted NO_2 transforms IO into INO_3 and subsequently deposits on aerosol surfaces, therefore, decreasing IO in most of the domain, especially along the ship tracks. Both $BrNO_3$ and INO_3 undergo photolysis and the photolysis rate of $BrNO_3$

Figure 4. Simulated monthly average of $ClNO_2$ (pptv, top), BrO (pptv, middle), and IO (pptv, bottom) at surface for the NO-SHIP (left) and FULL (center) scenarios. The relative change (in percentage) between scenarios is shown in the right column.

(Figure S4) is slower (hence regenerating less halogen atom or halogen oxide) than that of INO_3 (Figure S4). Such difference of photolysis rate between $BrNO_3$ and INO_3 induces a larger decrease in BrO than in IO (Figure 4). $ClNO_2$ is produced at night and can be transported to adjacent areas before being photolyzed at sunrise, therefore, the changes in $ClNO_2$ do not follow the ship tracks pattern as strictly as those in other halogen species. Note that the uptake of $ClNO_2$ on aerosols (when pH < 2) to form Cl_2 (Roberts et al., 2008) is not considered in the present work and is not expected to have noticeable influence because the simulated

pH is rarely lower than 2 in the bins with considerable sea-salt aerosol within our domain (Figure S5). On the contrary, BrO and IO are formed during the day and rapidly transform to other species (e.g., $BrNO_3$ and INO_3), therefore the suppressing effect of ship emissions is evident along the ship tracks.

3.3. Impact of Ship Emissions on the Halogens Partitioning

In this section, we investigate how ship emissions change the partitioning of halogen species. Figure 5 presents the monthly averaged percentage contribution of individual gaseous species to the total Cl_y, Br_y, and I_y in the NO-SHIP and FULL scenarios. For chlorine, ship emissions induce a shift from HOCl to Cl_2, mostly driven by heterogeneous recycling (Keene et al., 2009; Pechtl & von Glasow, 2007), and result in a less effective washout efficiency that increases the chlorine burden. In particular, including ship emissions reduces percentage contribution of individual species to Cl_y, that is, HOCl (from 71.8% to 50.3%), $ClNO_2$ (from 3.4% to 2.7%), BrCl (2.2% to 0.4%), and ICl (0.7% to 0.2%) and significantly increase that of Cl_2 (13.3% to 32.5%) and $ClNO_3$ (2.7% to 7.5%). Only small changes are induced to ClO and Cl. Note that the total abundance of chlorine species is increased with the addition of ship emissions (Figure 3) and such enhancement effect is stronger for some species than for others.

Shipping activities also affect the bromine partitioning, with the largest change in the $BrNO_3$ fraction from 5.2% to 16.2% and in BrO from 16.1% to 8.8%, due to the large emissions of NO_x transforming BrO into $BrNO_3$. BrCl is the dominant bromine fraction for both NO-SHIP and FULL schemes. Note that including the additional NO_x and SO_2 sources does not introduce a significant change in the sea-salt recycling of bromine (mainly driven by $BrNO_3$ and HOBr) as for the case of chlorine, where HOCl is the dominant fraction for the NO-SHIP case. The changes in iodine partitioning are similar to those of bromine species.

The average concentration and partitioning of halogen species during the daytime (8:00–17:00, local time) and nighttime (18:00–07:00, local time) in the NO-SHIP and FULL scenarios are depicted in Figures S6 and S7. The total chlorine and bromine abundances in the daytime are slightly higher than those in the nighttime, while total iodine during the day is lower compared to that at night in both NO-SHIP and FULL scenarios (Figures S6 and S7). The key changes of halogen partitioning between the NO-SHIP and FULL cases in the daytime (as well as the changes in the nighttime) are similar to those in daily average (Figure 5), for example, the decrease of HOCl, the increase of $BrNO_3$ and INO_3.

The partitioning of halogen species in the daytime shows distinct patterns compared to that at night (Figure S6 for the FULL scenario and Figure S7 for the NO-SHIP case). Here, we take the FULL case as an example. For daytime chlorine, the most abundant species is HOCl (59.7%) followed by Cl_2 (13.5%), $ClNO_3$ (13.7%), ClO (11.7%), etc., while at night, Cl_2 (48.2%) and HOCl (43.4%) contribute to most of the loading. For bromine species, HOBr (41.4%), $BrNO_3$ (23.8%), BrO (16.5%), and BrCl (9.8%) are the dominant daytime species, while at night the partitioning is dominated by BrCl (52.5%), IBr (21.9%), Br_2 (9.8%), and $BrNO_3$ (7.4%). In a global model study by Fernandez et al. (2014), HBr and HOBr are the species with elevated surface concentrations during the daytime in the Western Pacific (eastern part of the domain in present work), while Br_2, HBr, and BrCl are high at night. The present study does not show large levels of HBr because there are higher levels of pollutants, which activate the bromine from HBr (relatively more inert) to other more reactive species (e.g., via the reactions of $ClNO_3$ + HBr → BrCl, HOCl + HBr → BrCl, HBr + N_2O_5 → $BrNO_2$, and HOBr + HBr → Br_2). For the partitioning of iodine species in the daytime, HOI (66.2%), INO_3 (11.2%), and IO (15.0%) contribute more than 90% of total iodine, and HOI (59.5%), INO_3 (8.1%), I_2O_2 (9.6%), and I_2 (8.4%) take up most of the iodine at night. Saiz-Lopez et al. (2014) reported HOI as the most abundant species at noon at the surface in the tropics and dihalogen molecules (IBr + ICl + I_2) and HOI are the most abundant at midnight. Note that the reaction of HOI with NO_3 (Saiz-Lopez et al., 2016) is not included in the present work.

3.4. Impact of Halogens on Ship-Originated Air Pollutants

Figures 6 and 7 show the simulation of NO, NO_2, and O_3 in NO-HAL and the relative changes from NO-HAL to FULL. Halogens reduce both surface NO (on average by 9.6 pptv or 20.1%) and NO_2 (on average
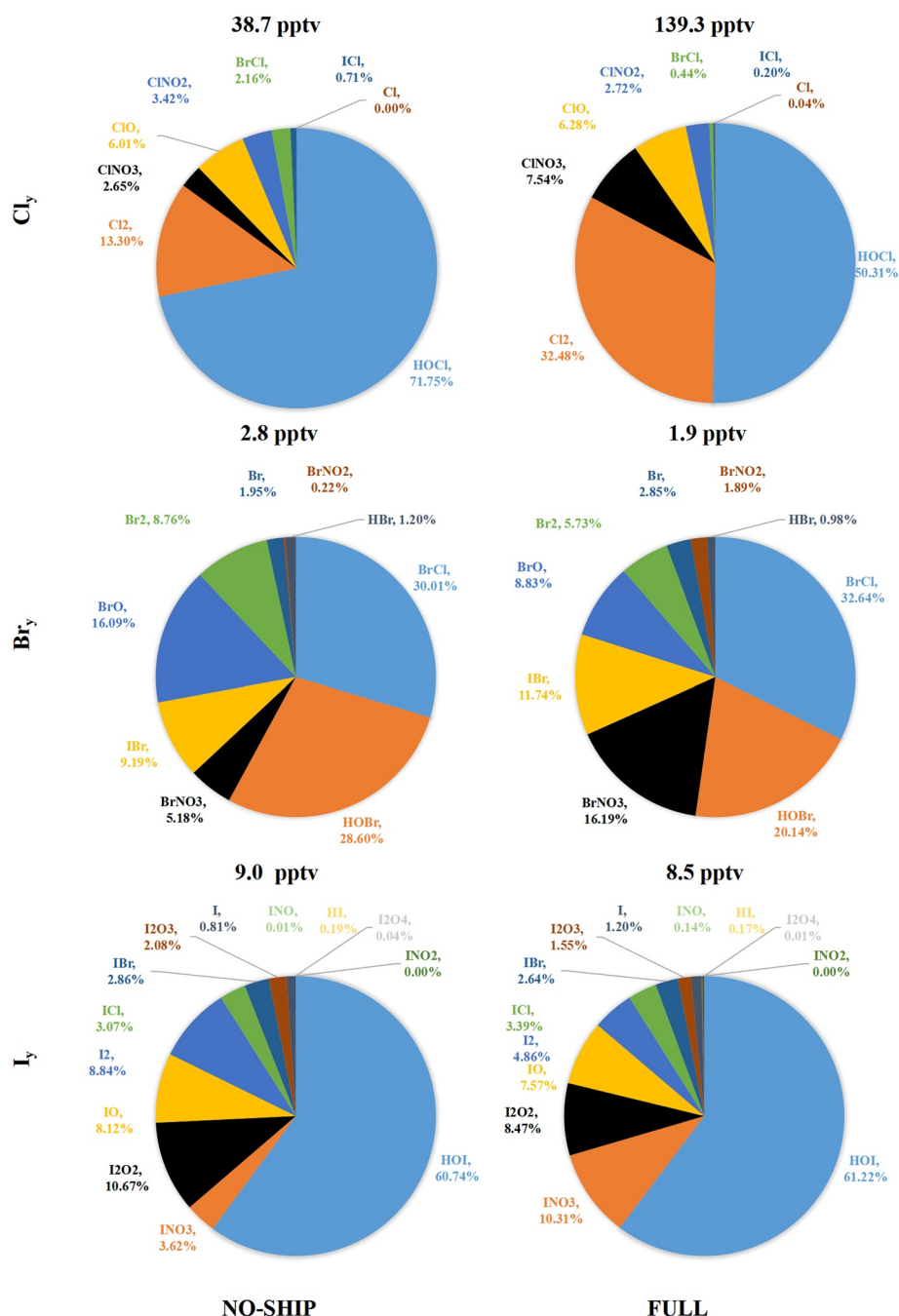
Figure 5. Partitioning of monthly average Cl_y (top), Br_y (middle), and I_y (bottom) for the NO-SHIP (left) and FULL (right) scenarios.

by 66.8 pptv or 18.7%) in most of the regions due to the transformation of NO_x to halogen nitrates, which ultimately form HNO_3 and deposit to the sea surface and aerosols. Note that along the ship tracks and close to the coast, NO is enhanced and NO_2 is reduced mostly because the loss of O_3 decreases the formation of NO_2 (from the reaction of $NO + O_3 \rightarrow NO_2$) resulting in an enhancement of NO. Li et al. (2019) applied the CMAQ model with comprehensive halogen chemistry in Europe and reported a decrease of NO_2 (as much as 1.7 ppbv) in the North Sea, the Mediterranean sea, and the polluted coastal areas and an increase of NO_2 (up to 0.20 ppbv) in other oceanic areas due to the same reason.
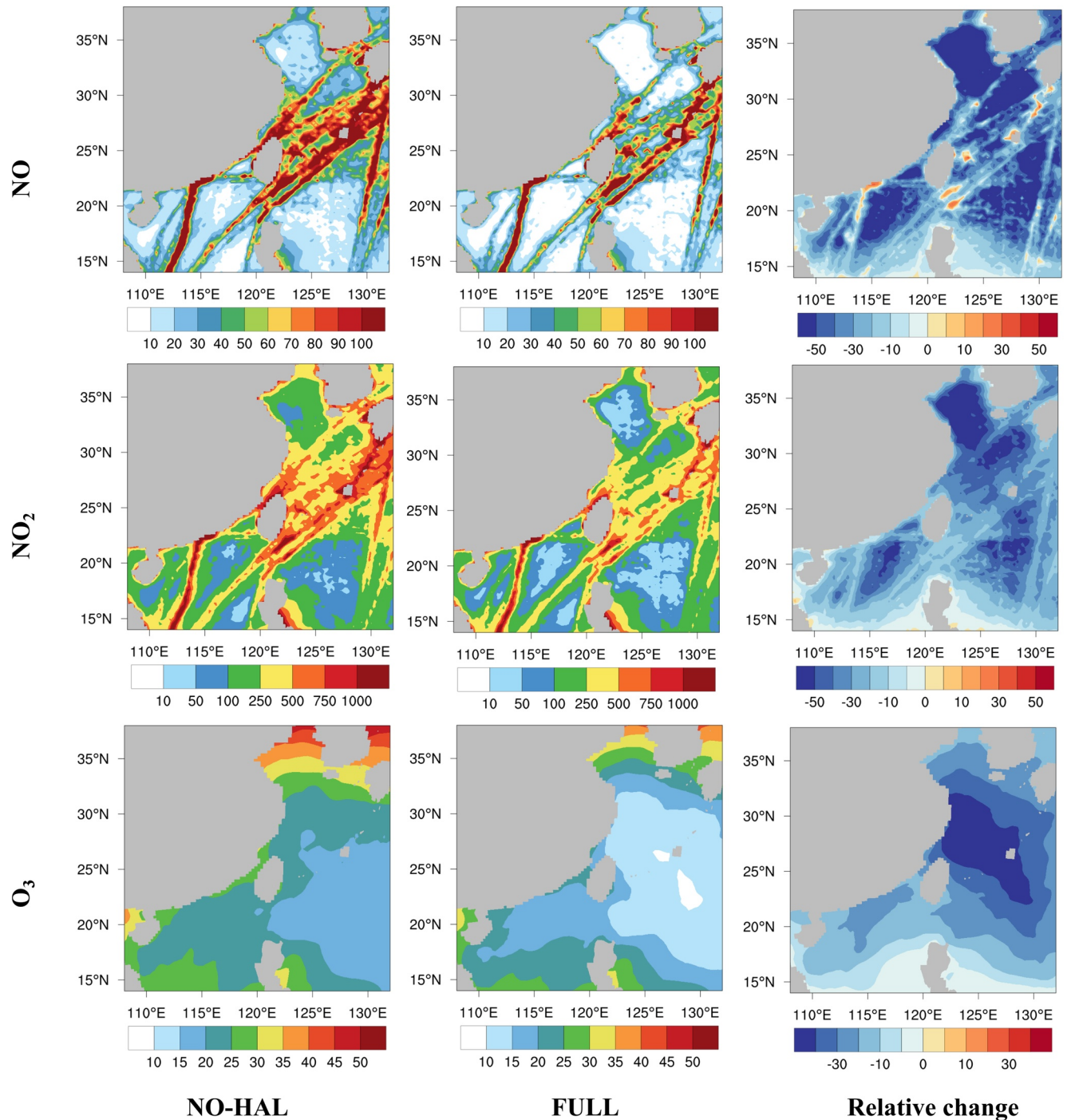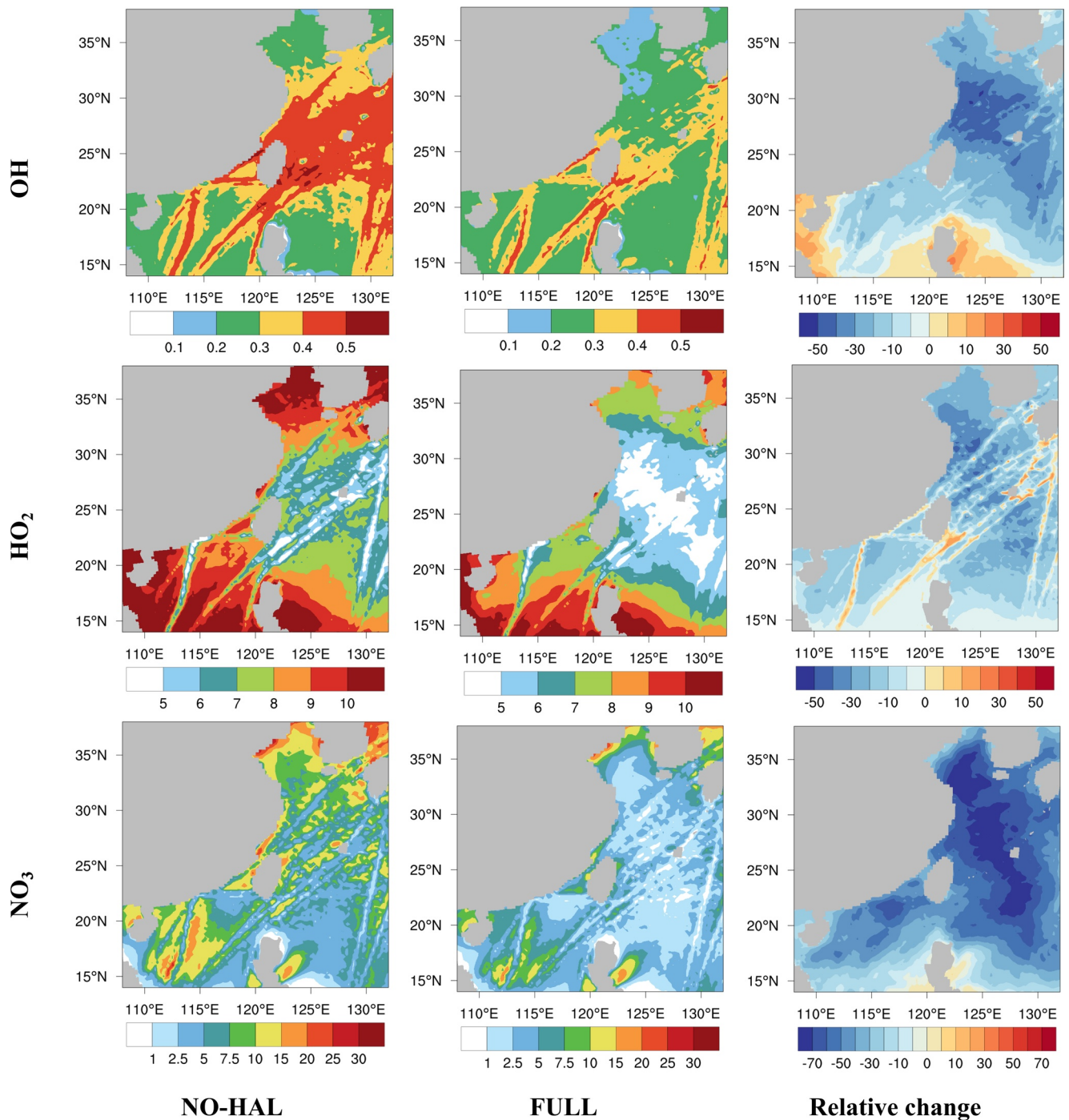
Figure 6. Simulated monthly average of NO (pptv, top), NO$_2$ (pptv, middle), and O$_3$ (ppbv, bottom) at the surface for the NO-HAL (left) and FULL (center) scenarios. The relative change (in percentage) between scenarios is shown in the right column.

Halogens consistently reduce the levels of O$_3$ (on average by 4.2 ppbv or 17.4%) throughout the domain because (1) halogen atoms directly destroy O$_3$, (2) halogen chemistry reduces the level of NO$_2$ and hence the production of O$_3$, and (3) the production of O$_3$ via the added reactions of Cl and Br atoms with VOCs is not able to compensate the enhanced loss of O$_3$ driven by (1) and the reduced production of O$_3$ driven by (2). Figure 7 shows a vertical perspective of the air pollutants for the NO-HAL and FULL cases along the latitudinal transect shown in Figure 1. Halogens reduce the NO$_x$ and O$_3$ throughout the MBL and even in the free
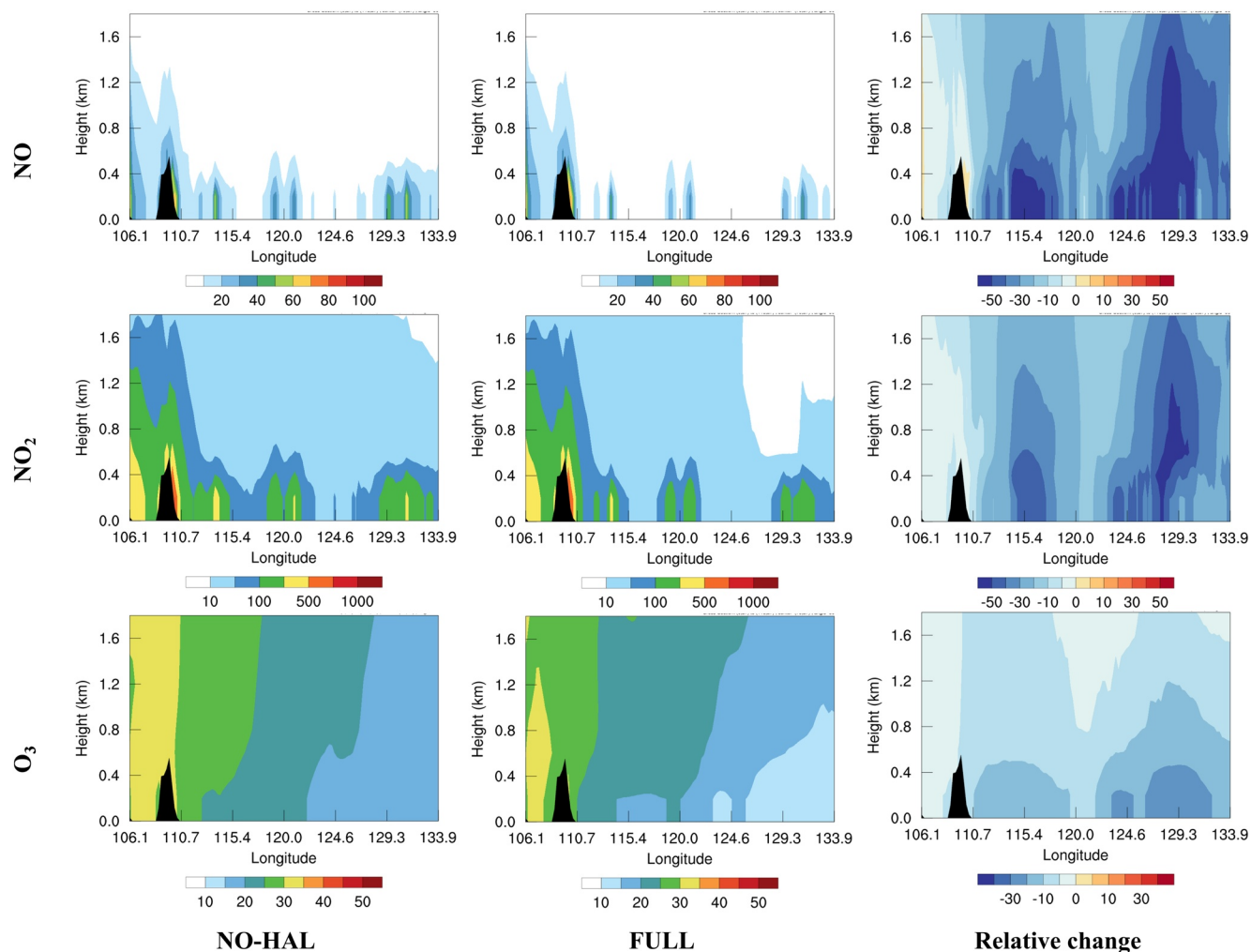
Figure 7. Simulated monthly average of NO (pptv, top), NO₂ (pptv, middle), and O₃ (ppbv, bottom) over the cross-section plane for the NO-HAL (left) and FULL (center) scenarios. The relative change (in percentage) between scenarios is shown in the right column. The black shared area corresponds to the location of the Hainan Island (see Figure 1).

troposphere, affecting the vertical transport of air pollutants (emitted over the continent and transported to the coastal and open ocean areas) from the surface to the MBL and the free troposphere. A hemispheric modeling study with CMAQ in the summer of 2006 (Sarwar et al., 2015) reported a reduction in O₃ of more than 6.0 ppbv in coastal areas because of halogens and >4.0 ppbv within the domain of the current study. Sherwen et al. (2016) and Sherwen, Schmidt, et al. (2016) utilized a global model (GEOS-Chem) and suggested that halogens reduced surface O₃ by ~10% (~a few ppbv) in the year of 2005 within the domain of the present work. A follow-up work of GEOS-Chem (Sherwen et al., 2017) reported a larger reduction of O₃ (as much as 28.9 ppbv) in July 2015 within the European domain. Muñiz-Unamunzaga et al. (2018) applied CMAQ in Los Angeles and found a decrease of 2.5–5.0 ppbv in O₃ along the coast in September 2006 due to the inclusion of full halogen chemistry. Sarwar et al. (2019) conducted a year-long simulation in 2006 of CMAQ and reported a decrease of 25% over oceanic waters and >6 ppbv in the present study domain. Li, Badia, Wang, et al. (2020) employed the WRF-Chem model to report 4%–10% reduction in surface O₃ along the coast in summer 2018 due to the addition of halogen sources and chemistry in China.

Figure 8. Simulated monthly average of OH (pptv, top), HO_2 (pptv, middle), and NO_3 (pptv, bottom) at the surface for the NO-HAL (left) and FULL (center) scenarios. The relative change (in percentage) between scenarios is shown in the right column.

3.5. Impact of Halogens on Free Radicals

The elevated levels of halogens in the presence of ship emissions (results in the FULL case as shown in Figure 3) in turn change the atmospheric composition with distinguished features along and around the ship tracks. Figure 8 illustrates the average spatial distribution of the main free radicals controlling atmospheric oxidation in the NO-HAL scenario, in the FULL scenario, and the relative changes.

In the NO-HAL case, the average levels of OH and HO_2 over the ocean are 0.32 pptv and 8.5 pptv, respectively. OH is higher along the ship tracks, while HO_2 is lower due to the emissions of NO from ships and the subsequent reaction of NO with HO_2 that transforms HO_2 into OH. The average NO_3 over the ocean is 7.1 pptv, with higher NO_3 outside the ship tracks compared to within the nearby tracks because the high levels of NO and NO_2 react with NO_3, reducing the levels of this radical.

Halogen chemistry decreases OH (on average by 0.05 pptv or 16.0%) and HO_2 (on average by 0.9 pptv or 10.8%) in most of the domain (Figure 8) because of significant O_3 destruction (Figure 6). Noticeably, in the grids with intensive ship emissions (Figure 1), OH is only slightly reduced and HO_2 is increased since halogens (mostly chlorine) increase the formation of HO_x via reactions of halogen atoms with ship-emitted VOCs (R5). NO_3 is formed through the reaction of NO_2 and O_3, and halogens decrease the NO_3 mixing ratios (on average by 2.8 pptv or 39.3%) because (1) halogens reduce the levels of NO_2; (2) halogens decrease O_3; (3) halogens directly react with NO_3 radical through the reactions of I_2 and I with NO_3. NO_3 concentration could be further decreased if the reaction of HOI with NO_3 (Saiz-Lopez et al., 2016) is included. The relative change of NO_3 due to halogens is not marked along the ship tracks (Figure 8) while the absolute change of NO_3 is evident along the tracks (Figure S8) because halogens induce the same decreasing effects on NO_3 (in contrast to the complex effects of halogens on HO_x) on and near the ship tracks. We also isolate the results in the daytime (for OH and HO_2) and nighttime (for NO_3) and the results show the same pattern (Figure S9).

Figure 9 shows the vertical cross-section results for the simulation of radicals in the NO-HAL and FULL scenarios and the corresponding changes. The effect of halogens on OH and HO_2 is higher below 400 m above sea level (a.s.l.), but a noticeable influence can be seen in the upper boundary layer and the free troposphere mostly due to the reduction of O_3. For NO_3, the decreasing effect due to halogens is more intense and reaches to more than 1,000 m a.s.l. because NO_x levels in addition to O_3 are significantly reduced.

Sarwar et al. (2015) used the CMAQ model to estimate that halogens led to an average decrease of OH (~1%) and HO_2 (~11%) in summer 2006 in the Northern Hemisphere. A global study with GEOS-Chem for the year of 2005 (Sherwen et al., 2016; Sherwen, Schmidt, et al., 2016) suggested a change of HO_x (OH + HO_2) in the range of -5% to 5% due to halogens within our domain. A follow-up work by Stone et al. (2018) found an increase of OH (~2%) and a decrease of HO_2 (-5% to -2%) for the year 2009 in East Asia. Li, Badia, Wang, et al. (2020) utilized the WRF-Chem model in China and reported changes of OH and HO_2 in between -10% and 20% in summer 2018 along the coast. Note that Li, Badia, Wang, et al. (2020) included anthropogenic chlorine emission over land for their simulation, which led to an increase of both OH and HO_2 in polluted coastal regions. Muñiz-Unamunzaga et al. (2018) used CMAQ model in Los Angeles and found a large decrease (-50% to -20%) in the NO_3 radical in September 2006 due to halogens and dimethyl sulfide chemistry. Li et al. (2019) suggested that halogen chemistry also significantly reduced the NO_3 levels by as much as 20 pptv in July 2016 in the Mediterranean Sea. Li, Badia, Wang, et al. (2020) estimated as much as a 30% decrease in NO_3 along the coast of China in summer 2018 due to halogen chemistry.

4. Conclusions and Final Remarks

This conceptual work exemplifies, on one hand, the impacts of shipping emissions on the atmospheric burden of RHS (increasing Cl_y by 260%, decreasing Br_y by 33%, and decreasing I_y by 6%) as well as on air pollutants and climate-relevant species (increasing NO_x by >100% and inducing a wide range of changes in O_3 from -16% to 23%) over the open ocean environment. On the other hand, our results account for the effects of RHS on the abundance and distribution of ship-originated free radicals (decreasing HO_x by more than 10% and decreasing NO_3 by ~40%) and air pollutants (decreasing NO_x by ~20% and decreasing O_3 by ~17%) in East Asia over the open ocean in summer. All of these highlight the importance of considering the long-range transport of oceanic natural sources interacting with anthropogenic pollutants not only in the vicinity of the ship tracks but also in the surrounding areas and vertically into the free troposphere.

Such chemical interaction between shipping emissions and RHS is also expected in other parts of the world with marked shipping activities, for example, the North Sea (Bencs et al., 2020), southern Europe (Nunes et al., 2020), northern Europe (Tang et al., 2020), and North Pacific and North Atlantic (Crippa et al., 2018).
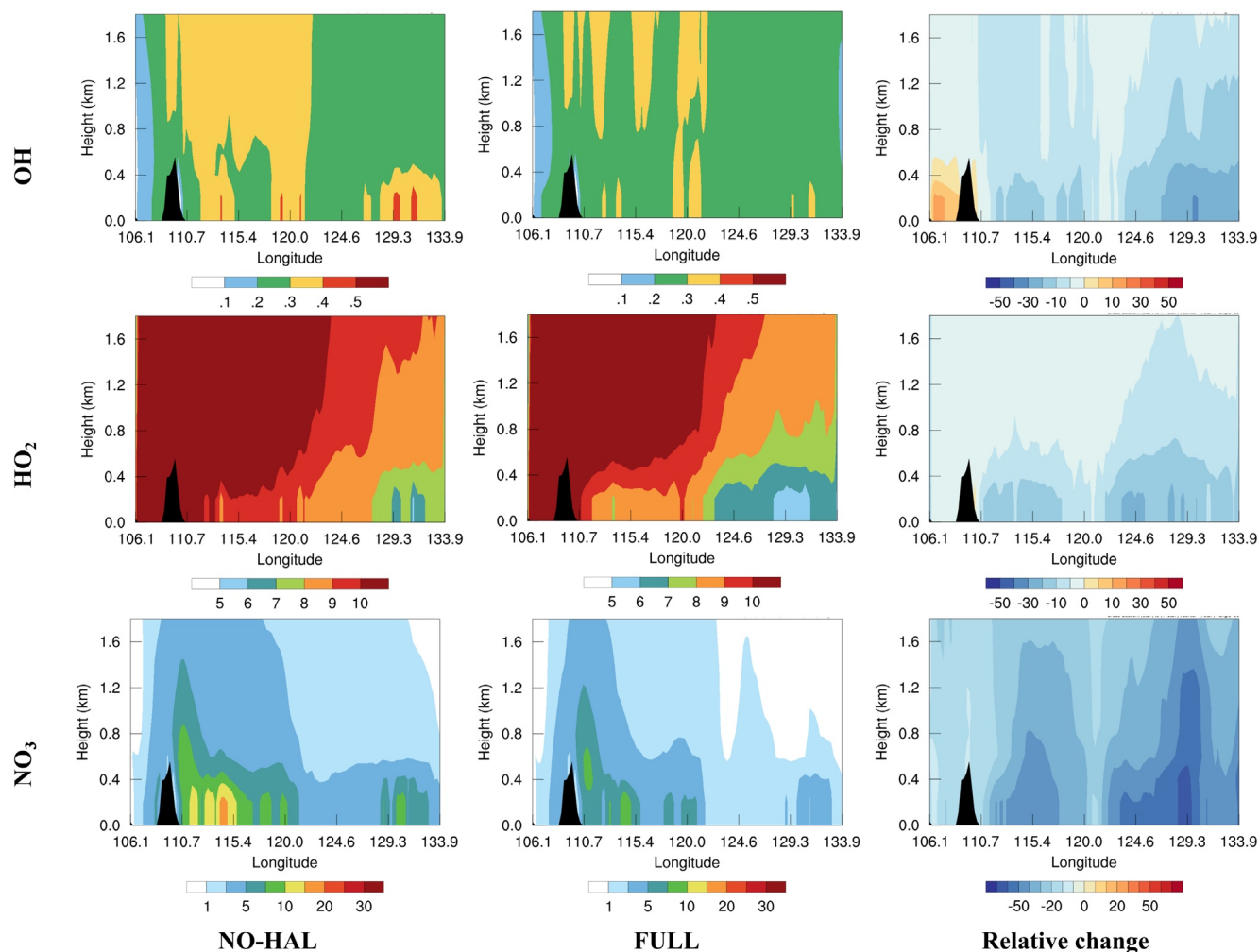
Figure 9. Simulated monthly average of OH (pptv, top), HO_2 (pptv, middle), and NO_3 (pptv, bottom) on the cross-section plane for the NO-HAL (left) and FULL (center) scenarios. The relative change (in percentage) between scenarios is shown in the right column.

While the chemical scheme and shipping emissions used in the present work are subject to some uncertainties as discussed in Sections 2 and 3, our analysis suggests that (1) ship emissions should be taken into account when studying reactive halogens from the ocean; (2) halogens should be considered when assessing the impact of shipping emission on air quality; and (3) further laboratory, field, and numerical modeling works are required to fully characterize the chemical interaction between ship emissions and oceanic halogens. A particular interest is to consider the synergistic interaction between shipping emissions and halogens on the regulation of air pollution for coastal cities with large ports, for example, Shanghai, Shenzhen, and Hong Kong. On a broader aspect, we recommend that the formulation of air quality and environmental policies should consider the strong chemical interaction between ship emissions and reactive halogen species.

Data Availability Statement

Data that support the finding of this study can be found at https://doi.org/10.17632/yd3bdrcwtb.1 (Li, Badia, Fernandez, et al., 2020).

References

Badia, A., Reeves, C. E., Baker, A. R., Saiz-Lopez, A., Volkamer, R., Koenig, T. K., et al. (2019). Importance of reactive halogens in the tropical marine atmosphere: A regional modelling study using WRF-Chem. *Atmospheric Chemistry and Physics*, *19*(5), 3161–3189. https://doi.org/10.5194/acp-19-3161-2019

Bencs, L., Horemans, B., Buczyńska, A. J., & Deutsch, F. (2020). Seasonality of ship emission related atmospheric pollution over coastal and open waters of the North Sea. *Atmospheric Environment X*, *7*, 100077. https://doi.org/10.1016/j.aeaoa.2020.100077

Carmichael, G. R., Tang, Y., Kurata, G., Uno, I., Streets, D. G., Thongboonchoo, N., et al. (2003). Evaluating regional emission estimates using the TRACE-P observations. *Journal of Geophysical Research*, *108*(D21), 8810. https://doi.org/10.1029/2002JD003116

Carpenter, L. J., MacDonald, S. M., Shaw, M. D., Kumar, R., Saunders, R. W., Parthipan, R., et al. (2013). Atmospheric iodine levels influenced by sea surface emissions of inorganic iodine. *Nature Geoscience*, *6*(2), 108–111.

Chen, D., Wang, X., Li, Y., Lang, J., Zhou, Y., Guo, X., & Zhao, Y. (2017). High-spatiotemporal-resolution ship emission inventory of China based on AIS data in 2014. *The Science of the Total Environment*, *609*, 776–787.

Chen, Y.-C., Christensen, M. W., Xue, L., Sorooshian, A., Stephens, G. L., Rasmussen, R. M., et al. (2012). Occurrence of lower cloud albedo in ship tracks. *Atmospheric Chemistry and Physics*, *12*, 8223–8235. https://doi.org/10.5194/acp-12-8223-2012

Crippa, M., Guizzardi, D., Muntean, M., Schaaf, E., Dentener, F., van Aardenne, J. A., et al. (2018). Gridded emissions of air pollutants for the period 1970–2012 within EDGAR v4.3.2. *Earth System Science Data*, *10*(4), 1987–2013. https://doi.org/10.5194/essd-10-1987-2018

Eyring, V., Isaksen, I. S. A., Berntsen, T., Collins, W. J., Corbett, J. J., Endresen, O., et al. (2010). Transport impacts on atmosphere and climate: Shipping. *Atmospheric Environment*, *44*(37), 4735–4771. https://doi.org/10.1016/j.atmosenv.2009.04.059

Fan, Q., Zhang, Y., Ma, W., Ma, H., Feng, J., Yu, Q., et al. (2016). Spatial and seasonal dynamics of ship emissions over the Yangtze River Delta and East China Sea and their potential environmental influence. *Environmental Science & Technology*, *50*(3), 1322–1329. https://doi.org/10.1021/acs.est.5b03965

Fernandez, R. P., Salawitch, R. J., Kinnison, D. E., Lamarque, J.-F. F., & Saiz-Lopez, A. (2014). Bromine partitioning in the tropical tropopause layer: Implications for stratospheric injection. *Atmospheric Chemistry and Physics*, *14*(24), 13391–13410. https://doi.org/10.5194/acp-14-13391-2014

Goren, T., & Rosenfeld, D. (2012). Satellite observations of ship emission induced transitions from broken to closed cell marine stratocumulus over large areas. *Journal of Geophysical Research*, *117*, D17206. https://doi.org/10.1029/2012JD017981

Großmann, K., Frieß, U., Peters, E., Wittrock, F., Lampel, J., Yilmaz, S., et al. (2013). Iodine monoxide in the Western Pacific marine boundary layer. *Atmospheric Chemistry and Physics*, *13*(6), 3363–3378. https://doi.org/10.5194/acp-13-3363-2013

Hatakeyama, S., Takami, A., Sakamaki, F., Mukai, H., Sugimoto, N., Shimizu, A., & Bandow, H. (2004). Aerial measurement of air pollutants and aerosols during 20–22 March 2001 over the East China Sea. *Journal of Geophysical Research*, *109*, D13304. https://doi.org/10.1029/2003JD004271

Hossaini, R., Chipperfield, M. P., Montzka, S. A., Rap, A., Dhomse, S., & Feng, W. (2015). Efficiency of short-lived halogens at influencing climate through depletion of stratospheric ozone. *Nature Geoscience*, *8*(3), 186–190. https://doi.org/10.1038/ngeo2363

Iglesias-Suarez, F., Badia, A., Fernandez, R. P., Cuevas, C. A., Kinnison, D. E., Tilmes, S., et al. (2020). Natural halogens buffer tropospheric ozone in a changing climate. *Nature Climate Change*, *10*, 147–154. https://doi.org/10.1038/s41558-019-0675-6

IMO. (2014). *Third IMO GHG study 2014*. London, UK: International Maritime Organization (IMO). http://www.imo.org/en/OurWork/Environment/PollutionPrevention/AirPollution/Pages/Greenhouse-Gas-Studies-014.aspx

Jacob, D. J., Crawford, J. H., Kleb, M. M., Connors, V. S., Bendura, R. J., Raper, J. L., et al. (2003). Transport and chemical evolution over the Pacific (TRACE-P) aircraft mission: Design, execution, and first results. *Journal of Geophysical Research*, *108*(20), 9000. https://doi.org/10.1029/2002JD003276

Keene, W. C., Long, M. S., Pszenny, A. A. P., Sander, R., Maben, J. R., Wall, A. J., et al. (2009). Latitudinal variation in the multiphase chemical processing of inorganic halogens and related species over the eastern North and South Atlantic Oceans. *Atmospheric Chemistry and Physics*, *9*, 7361–7385. https://doi.org/10.5194/acp-9-7361-2009

Koenig, T. K., Volkamer, R., Baidar, S., Dix, B., Wang, S., Anderson, D. C., et al. (2017). BrO and inferred Bry profiles over the western Pacific: Relevance of inorganic bromine sources and a Bry minimum in the aged tropical tropopause layer. *Atmospheric Chemistry and Physics*, *17*(24), 15245–15270. https://doi.org/10.5194/acp-17-15245-2017

Kontovas, C. A. (2020). Integration of air quality and climate change policies in shipping: The case of sulphur emissions regulation. *Marine Policy*, *113*(December 2019), 103815. https://doi.org/10.1016/j.marpol.2020.103815

Lan, Y. Y., Tsuang, B. J., Lin, N. H., Hsu, H. H., Yu, C. C., & Chen, Y. T. (2015). Distribution of ozone and related compounds in the marine boundary layer of the Northern South China Sea in 2010. *Aerosol and Air Quality Research*, *15*(5), 1990–2008. https://doi.org/10.4209/aaqr.2014.10.0242

Lawrence, M. G., & Crutzen, P. J. (1999). Influence of NO$_x$ emissions from ships on tropospheric photochemistry and climate, *Nature*, *402*, 167–170.

Li, Q., Badia, A., Fernandez, R. P., Mahajan, A. S., López-Noreña, A. I., Zhang, Y., et al. (2020). Chemical interactions between ship-originated air pollutants and ocean-emitted halogens. Mendeley Data, V1. https://doi.org/10.17632/yd3bdrcwtb.1

Li, Q., Badia, A., Wang, T., Sarwar, G., Fu, X., Zhang, L., et al. (2020). Potential effect of halogens on atmospheric oxidation and air quality in China. *Journal of Geophysical Research: Atmospheres*, *125*, e2019JD032058. https://doi.org/10.1029/2019JD032058

Li, Q., Borge, R., Sarwar, G., de la Paz, D., Gantt, B., Domingo, J., et al. (2019). Impact of halogen chemistry on summertime air quality in coastal and continental Europe: Application of the CMAQ model and implications for regulation. *Atmospheric Chemistry and Physics*, *19*(24), 15321–15337. https://doi.org/10.5194/acp-19-15321-2019

Li, Q., Zhang, L., Wang, T., Tham, Y. J., Ahmadov, R., Xue, L., et al. (2016). Impacts of heterogeneous uptake of dinitrogen pentoxide and chlorine activation on ozone and reactive nitrogen partitioning: Improvement and application of the WRF-Chem model in southern China. *Atmospheric Chemistry and Physics*, *16*(23), 14875–14890. https://doi.org/10.5194/acp-16-14875-2016

Liu, H., Fu, M., Jin, X., Shang, Y., Shindell, D., Faluvegi, G., et al. (2016). Health and climate impacts of ocean-going vessels in East Asia. *Nature Climate Change*, *6*(11), 1037–1041. https://doi.org/10.1038/nclimate3083

Liu, S., He, Z., & Yang, G. (2020). Bromoform, dibromochloromethane, and dibromomethane over the East China Sea and the western Pacific Ocean: Oceanic emission and spatial variation. *Chemosphere*, *257*, 127151. https://doi.org/10.1016/j.chemosphere.2020.127151

Liu, Z., Lu, X., Feng, J., Fan, Q., Zhang, Y., & Yang, X. (2017). Influence of ship emissions on urban air quality: A comprehensive study using highly time-resolved online measurements and numerical simulation in Shanghai. *Environmental Science & Technology*, *51*(1), 202–211. https://doi.org/10.1021/acs.est.6b03834

Lv, Z., Liu, H., Ying, Q., Fu, M., Meng, Z., Wang, Y., et al. (2018). Impacts of shipping emissions on PM 2.5 air pollution in China. *Atmospheric Chemistry and Physics*, *18*(21), 15811–15824. https://doi.org/10.5194/acp-18-15811-2018

Macdonald, S. M., Gómez Martín, J. C., Chance, R., Warriner, S., Saiz-Lopez, A., Carpenter, L. J., & Plane, J. M. C. (2014). A laboratory characterisation of inorganic iodine emissions from the sea surface: Dependence on oceanic variables and parameterisation for global modeling. *Atmospheric Chemistry and Physics*, *14*(11), 5841–5852. https://doi.org/10.5194/acp-14-5841-2014

Muñiz-Unamunzaga, M., Borge, R., Sarwar, G., Gantt, B., de la Paz, D., Cuevas, C. A., & Saiz-Lopez, A. (2018). The influence of ocean halogen and sulfur emissions in the air quality of a coastal megacity: The case of Los Angeles. *The Science of the Total Environment*, *610–611*, 1536–1545. https://doi.org/10.1016/j.scitotenv.2017.06.098

Nunes, R. A. O., Alvim-ferraz, M. C. M., Martins, F. G., Calderay-cayetano, F., Durán-grados, V., Moreno-gutiérrez, J., et al. (2020). Shipping emissions in the Iberian Peninsula and the impacts on air quality. *Atmospheric Chemistry and Physics Discussion*, *20*, 9473–9489.https://doi.org/10.5194/acp-2019-1186

Osthoff, H. D., Roberts, J. M., Ravishankara, A. R., Williams, E. J., Lerner, B. M., Sommariva, R., et al. (2008). High levels of nitryl chloride in the polluted subtropical marine boundary layer. *Nature Geoscience*, *1*(5), 324–328. https://doi.org/10.1038/ngeo177

Pechtl, S., & von Glasow, R. (2007). Reactive chlorine in the marine boundary layer in the outflow of polluted continental air: A model study. *Geophysical Research Letters*, *34*, L11813. https://doi.org/10.1029/2007GL029761

Prados-Roman, C., Cuevas, C. A., Hay, T., Fernandez, R. P., Mahajan, A. S., Royer, S. J., et al. (2015). Iodine oxide in the global marine boundary layer. *Atmospheric Chemistry and Physics*, *15*(2), 583–593. https://doi.org/10.5194/acp-15-583-2015

Roberts, J. M., Osthoff, H. D., Brown, S. S., & Ravishankara, A. R. (2008). N_2O_5 oxidizes chloride to Cl_2 in acidic atmospheric aerosol. *Science*, *321*(5892), 1059.

Saiz-Lopez, A., Fernandez, R. P., Ordóñez, C., Kinnison, D. E., Martín, J. C. G., Lamarque, J. F., & Tilmes, S. (2014). Iodine chemistry in the troposphere and its effect on ozone. *Atmospheric Chemistry and Physics*, *14*(23), 13119–13143. https://doi.org/10.1177/0964663912467814

Saiz-Lopez, A., Lamarque, J. F., Kinnison, D. E., Tilmes, S., Ordóñez, C., Orlando, J. J., et al. (2012). Estimating the climate significance of halogen-driven ozone loss in the tropical marine troposphere. *Atmospheric Chemistry and Physics*, *12*(9), 3939–3949. https://doi.org/10.5194/acp-12-3939-2012

Saiz-Lopez, A., Plane, J. M. C., Cuevas, C. A., Mahajan, A. S., Lamarque, J. F., & Kinnison, D. E. (2016). Nighttime atmospheric chemistry of iodine. *Atmospheric Chemistry and Physics*, *16*(24), 15593–15604. https://doi.org/10.5194/acp-16-15593-2016

Saiz-Lopez, A., & von Glasow, R. (2012). Reactive halogen chemistry in the troposphere. *Chemical Society Reviews*, *41*(19), 6448–6472. https://doi.org/10.1039/c2cs35208g

Sarwar, G., Gantt, B., Foley, K., Fahey, K., Spero, T. L., Kang, D., et al. (2019). Influence of bromine and iodine chemistry on annual, seasonal, diurnal, and background ozone: CMAQ simulations over the Northern Hemisphere. *Atmospheric Environment*, *231*, 395–404. https://doi.org/10.1016/j.atmosenv.2019.06.020

Sarwar, G., Gantt, B., Schwede, D., Foley, K., Mathur, R., & Saiz-Lopez, A. (2015). Impact of enhanced ozone deposition and halogen chemistry on tropospheric ozone over the Northern Hemisphere. *Environmental Science and Technology*, *49*(15), 9203–9211. https://doi.org/10.1021/acs.est.5b01657

Sarwar, G., Simon, H., Bhave, P., & Yarwood, G. (2012). Examining the impact of heterogeneous nitryl chloride production on air quality across the United States. *Atmospheric Chemistry and Physics*, *12*(14), 6455–6473. https://doi.org/10.5194/acp-12-6455-2012

Schreier, S. F., Peters, E., Richter, A., Lampel, J., Wittrock, F., & Burrows, J. P. (2015). Ship-based MAX-DOAS measurements of tropospheric NO_2 and SO_2 in the South China and Sulu Sea. *Atmospheric Environment*, *102*(2), 331–343. https://doi.org/10.1016/j.atmosenv.2014.12.015

Sherwen, T., Evans, M. J., Carpenter, L. J., Andrews, S. J., Lidster, R. T., Dix, B., et al. (2016). Iodine's impact on tropospheric oxidants: A global model study in GEOS-Chem. *Atmospheric Chemistry and Physics*, *16*(2), 1161–1186. https://doi.org/10.5194/acp-16-1161-2016

Sherwen, T., Evans, M. J., Sommariva, R., Hollis, L. D. J., Ball, S. M., Monks, P. S., et al. (2017). Effects of halogens on European air-quality. *Faraday Discussions*, *200*, 75–100. https://doi.org/10.1039/c7fd00026j

Sherwen, T., Schmidt, J. A., Evans, M. J., Carpenter, L. J., Großmann, K., Eastham, S. D., et al. (2016). Global impacts of tropospheric halogens (Cl, Br, I) on oxidants and composition in GEOS-Chem. *Atmospheric Chemistry and Physics*, *16*(18), 12239–12271. https://doi.org/10.5194/acp-16-12239-2016

Simpson, W. R., Brown, S. S., Saiz-Lopez, A., Thornton, J. A., & Von Glasow, R. (2015). Tropospheric halogen chemistry: Sources, cycling, and impacts. *Chemical Reviews*, *115*(10), 4035–4062. https://doi.org/10.1021/cr5006638

Stone, D., Sherwen, T., Evans, M. J., Vaughan, T., Whalley, L. K., et al. (2018). Impacts of bromine and iodine chemistry on tropospheric OH and HO_2: Comparing observations with box and global model perspectives. *Atmospheric Chemistry and Physics*, *18*(5), 3541–3561. https://doi.org/10.5194/acp-18-3541-2018

Tang, L., Ramacher, M. O., Moldanová, J., Matthias, V., Karl, M., Johansson, L., et al. (2020). The impact of ship emissions on air quality and human health in the Gothenburg area—Part I: 2012 emissions. *Atmospheric Chemistry and Physics Discussions*(2), 1–36. https://doi.org/10.5194/acp-2020-94

Travis, K. R., Heald, C. L., Allen, H. M., Apel, E. C., Arnold, S.R., Blake, D. R., et al. (2020). Constraining remote oxidation capacity with ATom observations. *Atmospheric Chemistry and Physics*, *20*(13), 7753–7781. https://doi.org/10.5194/acp-20-7753-2020

Von Schneidemesser, E., Monks, P. S., Allan, J. D., Bruhwiler, L., Forster, P., Fowler, D., et al. (2015). Chemistry and the linkages between air quality and climate change. *Chemical Reviews*, *115*(10), 3856–3897. https://doi.org/10.1021/acs.chemrev.5b00089

Wang, R., Tie, X., Li, G., Zhao, S., Long, X., Johansson, L., & An, Z. (2019). Effect of ship emissions on O_3 in the Yangtze River Delta region of China: Analysis of WRF-Chem modeling. *The Science of the Total Environment*, *683*, 360–370. https://doi.org/10.1016/j.scitotenv.2019.04.240

Wang, S., Hornbrook, R. S., Hills, A., Emmons, L. K., Tilmes, S., Lamarque, J. F., et al. (2019). Atmospheric acetaldehyde: Importance of air–sea exchange and a missing source in the remote troposphere. *Geophysical Research Letters*, *46*, 5601–5613. https://doi.org/10.1029/2019GL082034

Yang, X., Cox, R. A., Warwick, N. J., Pyle, J. A., Carver, G. D., O'Connor, F. M., & Savage, N. H. (2005). Tropospheric bromine chemistry and its impacts on ozone: A model study. *Journal of Geophysical Research*, *110*, D23311. https://doi.org/10.1029/2005JD006244

Zhang, Y., Yang, X., Brown, R., Yang, L., Morawska, L., Ristovski, Z., et al. (2017). Shipping emissions and their impacts on air quality in China. *The Science of the Total Environment*, *581–582*, 186–198. https://doi.org/10.1016/j.scitotenv.2016.12.098